euspen's 25th International Conference & Exhibition, Krakow, PL, June 2026
www.euspen.eu

Axial spindle deformation due to Poisson's effect under centrifugal loading

Byron R. Knapp, Dave Arneson, and Dan Oss

Professional Instruments Company, Hopkins, Minnesota, USA

bknapp@airbearings.com

Abstract

Centrifugal loading in high-speed ultra-precision spindles induces radial expansion of the rotor, which leads to micrometer-level axial shortening of the rotor through Poisson-coupled deformation. This work develops a finite element model to quantify speed-dependent axial displacement of an air-bearing spindle and validates the model experimentally. The spindle exhibits instantaneous micrometer-level axial contraction that increases approximately with the square of rotational speed, in agreement with analytical predictions. Experimental measurements reveal two distinct mechanisms of axial motion: a rapid elastic shortening due to centrifugal loading and a slower thermal drift arising from viscous shear heating of the air films. By applying linear drift removal, the thermal contribution is isolated, enabling direct comparison of the elastic response to model predictions. The corrected measurements and finite element model results agree within 3% at high speeds, demonstrating high fidelity of the modeling approach. The analysis further shows that the magnitude of axial deformation depends strongly on overhung length and attachments to the rotor, underscoring the importance of spindle design for high-speed applications. These validated results provide a foundation for real-time compensation of centrifugal-induced axial error in ultra-precision machining.

Air bearing design

1. Introduction

Increasing demands for deterministic machining of optical surfaces and molds require ultra-precision air bearing spindles capable of operating at higher rotational speeds for improved production efficiency [1]. Increasing spindle speed is a key strategy for enhancing machining productivity, reducing cycle times, and enabling the processing of brittle materials [2]. However, axial spindle motion directly affects tool position, cutting depth, and form errors, making micrometer-scale deviations unacceptable. High-speed spindle operation introduces two distinct axial error sources—axial thermal drift and induced axial deformation due to centrifugal loading—which may be misidentified despite occurring on fundamentally different time scales. In this paper, a model describing axial deformation induced by Poisson's effect under centrifugal loading in an ultra-precision air bearing spindle is developed and experimentally validated. To date, most published work on high-speed spindle error mechanisms has focused on thermal behavior [3,4], while comparatively little attention has been given to elastic deformation driven purely by centrifugal loading. Moreover, this effect becomes increasingly important for axial sensitive direction constant surface speed machining applications. In constant surface speed machining maintaining a fixed cutting velocity requires an increase in spindle speed as the cutting diameter decreases. Understanding and quantifying this deformation is therefore essential for developing accurate compensation strategies for next-generation ultra-precision machining systems.

2. Background

Centrifugal loading of a spindle rotor is a result of inertial forces that increase quadratically with rotational speed. These centrifugal forces cause radial expansion of the spindle as rotational speed increases. Due to the Poisson effect, radial expansion results in axial shortening even though there is no applied axial load. A rotor rotating with constant speed and unconstrained ends has zero axial stress but the axial strain ε_z is caused purely by the Poisson effect from the radial and tangential stresses:

$$\varepsilon_z = -\frac{\nu}{E}(\sigma_r + \sigma_t) \tag{1}$$

where ν is Poisson's ratio, E is Young's modulus, σ_r is the radial stress, and σ_t is the tangential (hoop) stress. This negative value indicates that the rotor contracts axially as it expands radially due to rotation.

Assuming a hollow cylinder of length L with inner radius r_i and outer radius r_o and density ρ the axial deformation δ_z is

$$\delta_z = \varepsilon_z \cdot L = -\frac{\nu\rho\omega^2(r_o^2+r_i^2)}{2E} \cdot L \tag{2}$$

Similarly, as the inner radius approaches zero, we have the following for the axial shortening of a solid cylinder

$$\delta_z = -\frac{\nu\rho\omega^2 r_o^2}{2E} \cdot L \tag{3}$$

Equations 1 and 2 can be used to estimate the axial deformation of a rotating shaft for the simple cases of solid and hollow shafts of constant cross-section. For more complex geometries, including multiple components attached to the spindle shaft, a finite element model must be used [5].

3. Finite element model

A finite element model is developed for the air bearing spindle shown in Figure 1 supported by experimental verification. The spindle features a captured thrust bearing positioned axially between two journal bearings, providing axial stiffness while the widely-spaced journal bearings provide radial and tilt stiffness. During operation at speeds up to 10,000 RPM, centrifugal effects induce instantaneous axial shortening that is directly proportional to the axial distance between the thrust bearing and the free end of the shaft, including any tooling, fixtures, or auxiliary components mounted to the shaft. Consequently, the axial placement of the thrust bearing and the effective overhung length of the shaft play a critical role in determining the magnitude of axial displacement due to centrifugal loading.

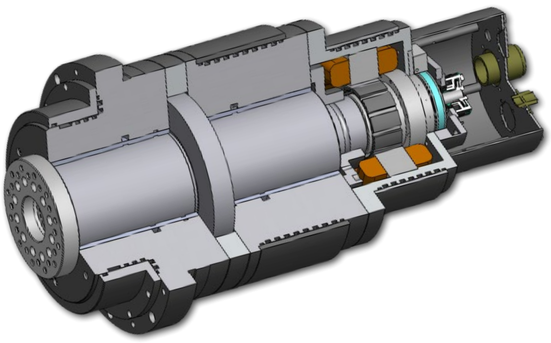

Figure 1. Professional Instruments ISO 5.5 air bearing spindle is the subject of this work.

Solidworks Simulation is used for the linear static analysis with the curvature-base mesher using solid elements and the h-adaptive solver. The model is reduced to a quarter-shaft representation (Figure 2) due to axis symmetry, decreasing computational cost and enabling application of the boundary conditions to prevent rigid-body motion of the model. Constraints are applied along the symmetry planes, resulting in two radial constraints normal to the symmetry planes and a third constraint applied in the axial direction normal to the thrust bearing surface.

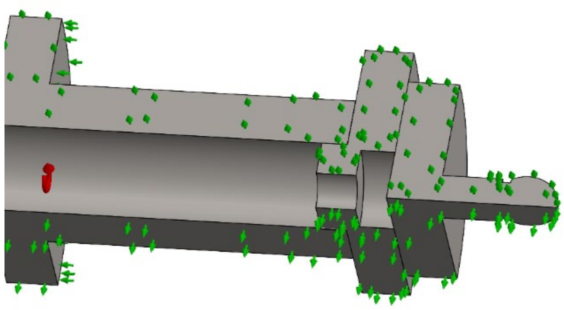

Figure 2. Finite element model of quarter shaft with boundary conditions and centrifugal loading.

To enable evaluation of axial deformation, a dedicated metrology surface is incorporated into the model. Specifically, a spherical testball is attached to the free end of the shaft, providing a well-defined geometric reference for axial displacement measurement. The complex geometry of the measurement hardware introduces some errors in the lumped model (Equations 1 and 2) due to the assumption of uniform axial strain. However, the axial strain is accurately predicted by the finite element analysis as shown in Figure 3.

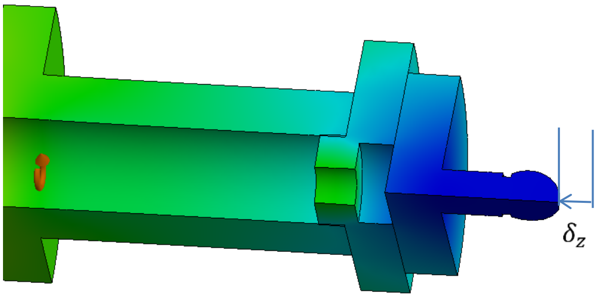

Figure 3. Finite element analysis showing axial displacement.

4. Experimental verification

To validate the finite element model, a series of controlled experiments were conducted to measure the axial displacement of the shaft of an ISO 5.5 air bearing spindle. Axial motion was measured using a non-contact capacitive displacement sensor with nanometer resolution (Lion Precision C23-C). As illustrated in Figure 4, the sensor was aligned with the axis of rotation and targeted a spherical artifact rigidly mounted to the rotor.

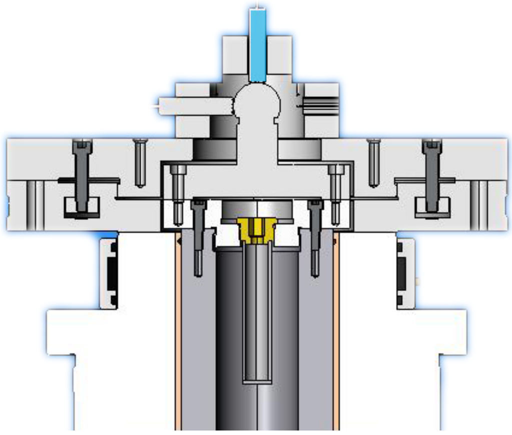

Figure 4. Setup to measure axial motion at speed.

Each experimental run followed a consistent speed profile. Starting from rest, the spindle was accelerated to a prescribed constant rotational speed, maintained at that speed for several seconds to allow transient effects to stabilize, and then decelerated to a complete stop. The resulting axial displacement of the shaft was recorded continuously throughout the entire cycle.

The measured response captures two distinct mechanisms contributing to axial motion as shown in Figure 5. First, the instantaneous axial displacement associated with centrifugal loading is observed during the acceleration and deceleration phases, corresponding to elastic deformation of the shaft and attached components. Second, a slower, time-dependent axial drift is evident during the constant-speed period. This drift is attributed to thermal effects arising from viscous shear of the air bearing films, which generates heat and produces axial expansion of the spindle structure. Over the short duration of the test, the thermal contribution is approximately linear with respect to time, allowing the centrifugal and thermal effects to be separated for comparison with model predictions.

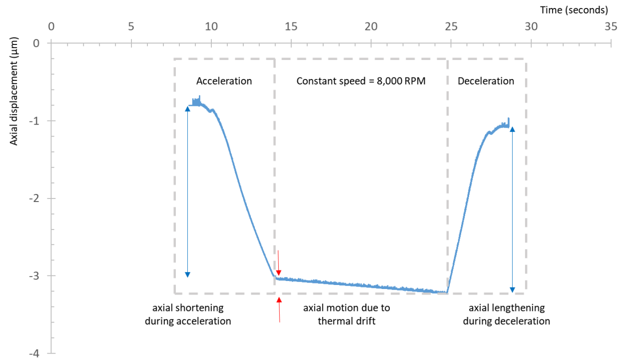

Figure 5. Axial displacement measurement before removal of thermal drift.

Measurement data similar to that presented in Figure 5 were collected over a range of spindle speeds from 500 RPM up to 10,000 RPM. For each test condition, axial displacement was recorded continuously throughout the acceleration, constant-speed, and deceleration phases. The test is conducted without liquid cooling and thermal expansion of the aluminum spindle housing is greater than the expansion of the stainless steel shaft, resulting in thermal displacement in the negative direction. To isolate the elastic response of the shaft, the time-dependent thermal component was removed from each data set by fitting and subtracting a linear trend, as illustrated in Figure 6. This approach is justified by the approximately linear thermal drift observed over the short duration of each test.

Following removal of the thermal contribution, the remaining axial displacement is dominated by the elastic deformation of the shaft under centrifugal loading. The resulting axial shortening increases with spindle speed and exhibits the expected symmetry during acceleration and deceleration, providing a clear experimental signature of the centrifugal loading mechanism. The processed data therefore enable direct comparison with finite element predictions of speed-dependent axial deformation.

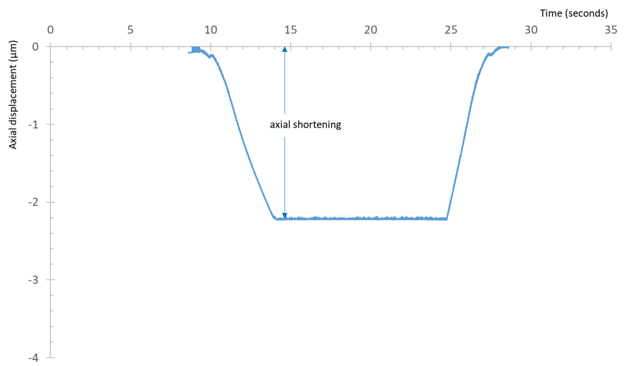

Figure 6. Axial displacement measurement after removal of thermal drift.

5. Results

The finite element model developed for the spindle rotor assembly shows strong predictive capability for the axial deformation induced by centrifugal loading, and these predictions are in close agreement. Figure 7 presents the comparison between modeled and measured axial shortening after removal of the thermally induced drift component. The finite element model results confirm that axial contraction increases approximately with the square of rotational speed, consistent with the analytical trends predicted by Equations 2 and 3. At low rotational speeds (less than 5,000 RPM), both the modeled and measured axial displacements are relatively small, approaching the noise floor of the measurement. As speed increases, however, the deformation becomes clearly measurable, and by 10,000 RPM the spindle exhibits 3.5 µm of instantaneous axial shortening. This behavior reflects the combined influence of radial and tangential stress components in the shaft and attached tooling, which drive the Poisson-induced axial contraction predicted by the model.

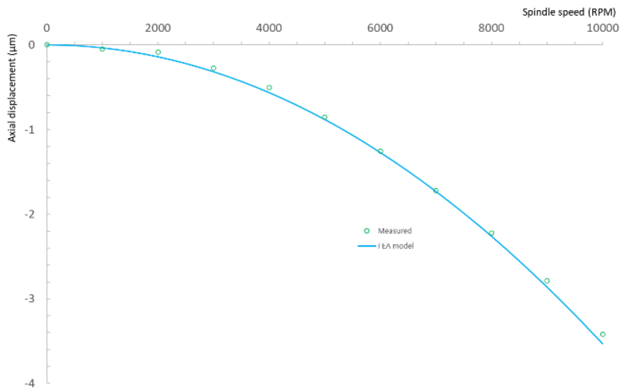

Figure 7. Verification of the modeled axial displacement versus speed.

The experimental measurements clearly reveal two distinct timescales of axial motion:

- Instantaneous deformation occurring during acceleration and deceleration, driven by centrifugal loading of the shaft.
- Time-dependent drift occurring during constant-speed operation, attributed to thermal expansion caused by viscous air-film shear heating.

Following linear removal of thermal drift from the experimental data, the measured elastic response closely tracks the finite element model predictions. Above 5,000 RPM, where the deformation signal is well separated from measurement noise, the difference between the modeled and measured axial shortening remains within 3%, demonstrating excellent quantitative agreement. This level of correlation validates the modeling assumptions and confirms that the dominant mechanism—centrifugal radial expansion coupled through Poisson's effect—is accurately captured by the finite element analysis.

6. Discussion

The agreement between model and experiment demonstrates that centrifugal-induced axial shortening is a predictable and significant contributor to axial motion in high-speed ultra-precision spindles. A key implication of this work is the impact of centrifugal deformation on machining applications with axial sensitive direction that employ constant surface speed cutting. Since the spindle speed must continuously increase as cutting diameter decreases, the dynamic change in spindle speed introduces an accompanying speed-dependent axial shift that directly affects cutting depth and form accuracy.

The results presented here show that axial shortening scales approximately with the square of spindle speed, meaning that deformation increases rapidly when diameters are smallest and rotational speeds are highest. Without compensation, this can introduce micrometer-level form deviations—an unacceptable outcome for applications requiring sub-100 nm accuracy. This phenomenon is especially relevant for spindles with long overhung lengths and fixtures attached to the rotor that magnify the axial displacement induced by centrifugal loading.

The findings indicate that axial tool-position error during high-speed or constant surface speed machining can be estimated and compensated in real time using spindle speed. Since the elastic response is instantaneous and reversible, integration of a predictive model—such as the finite element framework validated here—into the machine control system would allow direct correction of the axial tool position as speed changes. Such compensation becomes even more critical when combined with thermal drift, which evolves on a slower timescale but can obscure the underlying elastic behavior if uncorrected.

Overall, the validated finite element model provides not only physical insight into Poisson-driven axial shortening but also a practical foundation for implementing real-time compensation strategies. As machining systems continue to pursue higher throughput, smaller feature sizes, and more aggressive machining strategies, accounting for centrifugal deformation will become increasingly essential for achieving deterministic accuracy in ultra-precision manufacturing.

7. Conclusion

This work demonstrates that centrifugal loading in high-speed ultra-precision spindles produces measurable axial shortening through Poisson-coupled radial expansion, and that this elastic deformation is both instantaneous and strongly dependent on rotational speed. A finite element model was developed to quantify this behavior for a practical air-bearing spindle, and experimental measurements confirmed the predicted speed-dependent response. After removal of the slower thermal drift component, the measured axial shortening agreed with the model within 3% at high speeds, validating the accuracy of the modeling approach.

The results show that axial deformation scales approximately with the square of spindle speed, making it increasingly significant in machining strategies—such as constant surface speed cutting—that require continuous acceleration as tool diameter decreases. This speed-induced axial shift can introduce micrometer-level form errors if not properly accounted for. Because the elastic response is instantaneous and reversible, the validated model provides a practical basis for real-time compensation of speed-dependent tool-position error.

Overall, this work establishes both the physical mechanism and quantitative magnitude of centrifugal-induced axial shortening in ultra-precision spindles, and it provides a predictive framework that can be directly integrated into next-generation machining systems to improve accuracy in high-speed and constant-surface-speed applications.

References

[1] E Brinksmeier and L Schönemann (Eds.) Ultra-precision High Performance Cutting. Report of DFG Research Unit FOR 1845. Springer Nature Switzerland AG Cham: 2020.

[2] M Tunesi et al. Effect of cutting speed in single point diamond turning of (100)Ge. Manufacturing Letters. 38: 15-18, 2023.

[3] H Yoshioka et al. Minimizing thermal deformation of aerostatic spindle system by temperature control of supply air. JSME Intl. C. 49: 606-611, 2006.

[4] S Rakuff and P Beaudet. Thermally induced errors in diamond turning of optical structured surfaces. Optical Engineering. 46:10, 2007.

[5] K Yokoyama. Analysis of deformation of air-spindle due to centrifugal force. J of JSPE. 64:1,137-141, 1998.